Study on the Second Dissociation Channel of CS_2^+ by Using [1+1] Two-Photon Dissociation

Limin Zhang,* Feng Wang, Zhong Wang, Shuqin Yu, Shilin Liu, and Xingxiao Ma

Laboratory of Bond Selective Chemistry, Department of Chemical Physics, University of Science and Technology of China, Hefei, Anhui 230026, People's Republic of China

Received: September 20, 2003; In Final Form: December 11, 2003

The second dissociation channel ($CS_2^+ \rightarrow CS^+(X\ ^2\Sigma) + S(^3P)$) of CS_2^+ molecular ions has been investigated by measuring the photofragment CS^+ excitation (PHOFEX) spectrum in the wavelength range of 385−435 nm, where the CS_2^+ molecular ions were prepared purely by [3 + 1] multiphoton ionization of the neutral CS_2 molecules at 483.2 nm. The CS^+ PHOFEX spectrum was assigned essentially to the CS_2^+ ($\tilde{A}^2\Pi_u$) ← CS_2^+ ($\tilde{X}^2\Pi_g$) transition, such as the S^+ PHOFEX spectrum, which has been obtained previously. The product branching ratios (CS^+/S^+), as measured from the PHOFEX spectra, increase from 0 to slightly larger than 1 in the wavenumber range of 47200−50400 cm^{-1}. The adiabatic appearance potential of the CS^+ ion was determined to be 5.852 ± 0.005 eV above the $\tilde{X}^2\Pi_{g,3/2}$ (0,0,0) level of CS_2^+ from the appearance wavenumber of 47196.2 cm^{-1} to produce the CS^+ ion. The dissociation mechanism to get to CS^+ + S from CS_2^+ was discussed and preliminarily attributed to (i) CS_2^+ ($\tilde{X}^2\Pi_g$) → CS_2^+ ($\tilde{A}^2\Pi_u$) through one-photon excitation, (ii) CS_2^+ ($\tilde{A}^2\Pi_u$) → CS_2^+ ($\tilde{X}^\dagger$) via internal conversion process due to the vibronic coupling between the $\tilde{A}$ and $\tilde{X}$ states, (iii) CS_2^+ ($\tilde{X}^\dagger$) → CS_2^+ ($\tilde{B}^2\Sigma_u^+$) through the second photon excitation, and (iv) CS_2^+ ($\tilde{B}^2\Sigma_u^+$) → $CS^+(X\ ^2\Sigma) + S(^3P)$, because of the potential curve crossing with the repulsive $^4\Sigma^-$ state and/or the $^2\Sigma^-$ state correlated with the second dissociation limit.

Introduction

As an important molecule in astrophysics and atmospheric physics,[1] the CS_2^+ ion has been the subject of extensive study. Previously, many investigators have studied experimentally the spectrum and the dissociation dynamics of CS_2^+.[2−24] The development of sophisticated new experimental methods, which often involved several lasers, has made it possible to study the fragmentation mechanism of CS_2^+ in unprecedented precision. From such experiments, one can derive information concerning the excitation mechanism, the internal energy transfer within the excited complex, and the actual bond rupture.

In addition to the three bound electronic states of $\tilde{X}$, $\tilde{A}$, and $\tilde{B}$ of CS_2^+,[4,5] the higher excited state, which is called $\tilde{C}^2\Sigma_g^+$, was observed from the photoelectron spectroscopy[6−8] and studied further by Frey et al.[10] and Wang et al.[11] to determine the vibrational frequencies. The $\tilde{C}^2\Sigma_g^+$ state was determined to be fully predissociative and correlated with both S^+ + CS and S + CS^+ fragments.[20] Momigny et al.[12] proposed a model to account for the metastable levels in CS_2^+ that lead to $S^+(^4S)$ + $CS(X\ ^1\Sigma^+)$ and $CS^+(X\ ^2\Sigma)$ + $S(^3P)$ under the electron impact on CS_2 molecules, in which the curve crossing from the $\tilde{C}^2\Sigma_g^+$ state to a fully repulsive $^4\Sigma^-$ state or/and a repulsive $^2\Sigma^-$ state should be responsible for the predissociation. The dissociation dynamics in the $\tilde{C}^2\Sigma_g^+$ state was studied in detail by Maier and co-workers[21,22] and recently by Hwang et al.,[23] using a two-color optical−optical double resonance method. These works had determined the predissociative lifetimes and the CS^+/S^+ branching ratios, as well as the average kinetic energy releases for several vibrational levels in the $\tilde{C}$ state. Although it was proposed that[12] the curve crossing from the $\tilde{C}^2\Sigma_g^+$ state to a fully repulsive $^4\Sigma^-$ state or/and a repulsive $^2\Sigma^-$ state should be responsible for the predissociation in CS_2^+ that leads to $S^+(^4S)$ + $CS(X\ ^1\Sigma^+)$ and $CS^+(X\ ^2\Sigma)$ + $S(^3P)$, the following questions concerning the dissociation in CS_2^+ still remain to be answered: (i) is the predissociation in CS_2^+ that leads to $CS^+(X\ ^2\Sigma)$ + $S(^3P)$ required to occur via the $\tilde{C}^2\Sigma_g^+$ state? and (ii) where is the adiabatic appearance potential to the second dissociation limit $CS^+(X\ ^2\Sigma)$ + $S(^3P)$ of CS_2^+?

Recently, the photoelectron−photoion coincidence (PEPICO) spectroscopy of CS_2 by Aitchison and Eland[29] showed that the CS^+ product ion appears at ∼15.8 eV above the $CS_2(\tilde{X}(000))$ level, which is lower than the $CS_2^+(\tilde{C}^2\Sigma_g^+(000))$ level at 16.188 eV.[30] However, the best way to answer the aforementioned questions is dependent on the direct excitation of the CS_2^+ molecular ion. In this report, the second dissociation channel ($CS_2^+ \rightarrow CS^+(X\ ^2\Sigma) + S(^3P)$) of the CS_2^+ molecular ion is investigated by measuring the photofragment CS^+ excitation (PHOFEX) spectrum in the wavelength range of 385−435 nm, where the two-photon energy crosses the energy position of the $\tilde{C}^2\Sigma_g^+$ state. According to the model proposed by Momigny et al.,[12] both the $^4\Sigma^-$ repulsive state (which correlates with the first dissociation limit $S^+(^4S)$ + $CS(X^1\Sigma^+)$) and the second dissociation limit $CS^+(X\ ^2\Sigma)$ + $S(^3P)$) and the $^2\Sigma^-$ repulsive state (which correlates only with the second dissociation limit $CS^+(X^2\Sigma)$ + $S(^3P)$) crosses the $\tilde{X}^2\Pi_g$, $\tilde{A}\ ^2\Pi_u$, and $\tilde{B}^2\Sigma_u^+$ states at their highly excited vibrational levels. If this is really the case, CS_2^+ cations that are lying at high vibrational levels in the $\tilde{B}^2\Sigma_u^+$ state should be predissociative. However, because of the narrow Franck−Condon contour for the $\tilde{B}^2\Sigma_u^+ - \tilde{X}^2\Pi_g$ transition,[13] direct excitation from the ground state $\tilde{X}\ ^2\Pi_g$ to the high vibrational levels in the $\tilde{B}$-state is improbable. Therefore, an intermediate state is necessary to pump through to the high vibrational levels in the $\tilde{B}$-state.

In our previous study,[2] we investigated the photodissociation of CS_2^+ ions via the first dissociation channel to S^+ + CS through two-photon resonant excitation. In this report, as the continuation of our previous study, we prepared the CS_2^+ ions

* Author to whom all correspondence should be addressed. E-mail: lmzha@ustc.edu.cn.

10.1021/jp036820q CCC: $27.50
Published on Web 02/03/2004

cleanly by [3+1] REMPI through the 4p Rydberg state at a wavelength of 483.2 nm,[25,26] and excited the CS_2^+ ions by [1+1] two-photon resonant excitation via the intermediate bound state $\tilde{A}^2\Pi_u$ in the wavelength range of 385−435 nm. From the S^+ and CS^+ fragment PHOFEX spectra of CS_2^+ ions that was observed, the adiabatic appearance potential of the CS^+ ion was deduced and the excitation and dissociation processes to form CS^+ fragments were investigated.

Experiment

The experimental setup has been reported previously.[2] Briefly, it consists of (i) a pulsed molecular beam source to generate the jet-cooled CS_2 molecules, (ii) two dye-laser systems pumped by two YAG lasers, each with a pulse width of ∼5 ns, and (iii) a homemade time-of-flight (TOF) mass spectrometer.

The jet-cooled CS_2 molecules were produced by the supersonic expansion of a CS_2/helium gas mixture (CS_2/helium ≈ 5%) through a pulsed nozzle (General Valve) with a nozzle orifice diameter of 0.5 mm into a photoionization chamber. The laser-molecule interaction region was located 6 cm downstream from the nozzle orifice. The TOF mass spectrometer was pumped by two turbomolecular pumps, with flow rates of 500 L/s and 450 L/s. The stagnation pressure was kept at ∼3 atm, and the operating pressures in the interaction region were 2×10^{-5} Torr.

One dye laser (Model FL3002, Lambda Physics) that was pumped by the THG (354.7 nm) output of a Nd:YAG laser (LABest Optronics) was used for photoionization. The output of the photoionization dye laser (483.2 nm, ∼1.5 mJ/pulse) was focused perpendicularly on the molecular beam of CS_2 by a quartz lens with $f = 150$ mm and was used to prepare CS_2^+ molecular ions via [3+1] REMPI of CS_2. The photodissociation dye laser, with the output of ∼0.1 mJ/pulse in the range of 385−485 nm was used to dissociate the CS_2^+ ions via [1+1] two-photon excitation. This light was coaxially counterpropagated with the photoionization laser and weakly focused by another quartz lens with a focal length of $f = 600$ mm. Both dye lasers were temporally and spatially matched with each other at the laser-molecular interaction point. The wavelength of the laser was calibrated by a neon hollow-cathode lamp.

The produced ions, including the parent CS_2^+ ions and the fragment ions, were extracted and accelerated into a TOF mass spectrometer and drifted along a 70-cm-long TOF tube, and they were finally detected by a microchannel plate (MCP) detector. The signals from the MCP output were amplified with a preamplifier (NF, BX-31), and the mass-resolved data were collected by averaging the amplified signals for selected mass species with boxcar averagers (Stanford Model SR250) and then interfaced to a personal computer (PC) for data storage. The intensities of the ionization laser and the photodissociation laser were monitored simultaneously during the experiment.

Results and Discussion

(A) Photofragment Excitation Spectrum. Fixing the wavelength of the ionization laser at $\lambda = 483.2$ nm, we could certainly prepare exclusive CS_2^+ ions in the $\tilde{X}^2\Pi_g$ state with a minimum amount of S^+ and CS^+ ions,[2] using a lens with a middle focus length of $f = 150$ mm and optimizing the pulse energy of the ionization laser at ∼1.5 mJ. This observation means that we can achieve the soft ionization using the present ionization scheme of [3+1] REMPI of CS_2 at this wavelength;[25] that is,

$$CS_2(\tilde{X}\,^1\Sigma_g^+) \xrightarrow{3h\nu} CS_2(4p\,\sigma\,^3\Pi_u) \xrightarrow{h\nu} CS_2^+(\tilde{X}\,^2\Pi_g) + e$$

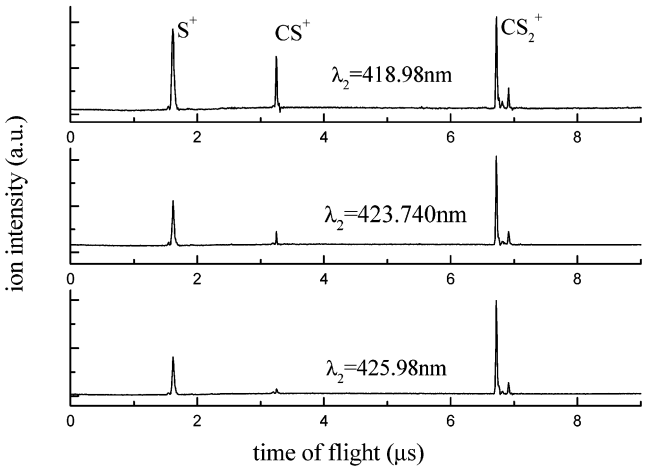

Figure 1. Time-of-flight (TOF) mass spectra obtained with the ionization laser wavelength λ_1 fixed at 483.2 nm and the dissociation laser wavelengths λ_2 at 418.98, 423.74, and 425.98 nm.

With the elimination of any obvious interference from the background ions, the photodissociation mechanism of the CS_2^+ ions can be investigated by introducing the photodissociation laser. By carefully controlling the intensity of the dissociation laser, no ion signal could be observed only with this laser in the wavelength range of $\lambda = 385-435$ nm; however, the remarkably strong S^+(385−435 nm) and CS^+(385−424 nm) signal appeared in the TOF mass spectrum with both the ionization laser and the dissociation laser. The S^+ and CS^+ ions were confirmed to be generated completely from the interaction of the dissociation laser on the parent molecular CS_2^+ ions, by varying the temporal delay and the spatial overlap between the two lasers. To avoid disturbance from the autoionization of neutral CS_2, there was an ∼60 ns delay temporally and a slight separation in the direction of ion flight between the dissociation laser and the ionization laser in the laser-molecule interaction region. Figure 1 shows the action TOF mass spectrum with both the ionization laser ($\lambda_1 = 483.2$ nm) and the dissociation laser ($\lambda_2 = 418.98$, 423.74, and 425.98 nm, respectively), which were matched spatially and temporally with each other. The mass spectrum in Figure 1 shows that a remarkably strong CS^+ signal appears only with $\lambda_2 = 418.98$ nm but a strong S^+ signal appears with all three λ_2 values of the dissociation laser.

The one-photon excitation energy can access neither the first dissociation limit ($S^+(^4S)$+ $CS(X^1\Sigma^+)$) nor the second dissociation limit ($CS^+(X\ ^2\Sigma)$ + $S(^3P)$) of the CS_2^+ ion from its electronic ground state;[12] therefore, the [1+1] two-photon excitation of the parent CS_2^+ ions by the dissociation laser (i.e., excitation from the electronic ground state to an intermediate state and then to a dissociative state) is needed to produce S^+ and CS^+ ions. A scan of the dissociation laser while monitoring the S^+ and CS^+ ions enabled us to obtain PHOFEX spectra, which contain information related to the two sequential transitions. Therefore, the spectroscopic information on the intermediate state, as well as the dissociation mechanism, can be obtained from the spectrum. Figure 2 shows the PHOFEX spectrum by monitoring S^+ ions in the wavelength range of 385−482 nm.[2] With the aid of the spectroscopic data obtained from previous studies on the spectroscopy of CS_2^+,[2,4,9,10,13,24] this PHOFEX spectrum could be assigned completely as the radiative electronic transition $CS_2^+(\tilde{A}^2\Pi_u) \leftarrow CS_2^+(\tilde{X}^2\Pi_g)$. This observation means that the intermediate state in the [1+1] dissociation process to generate S^+ is the $\tilde{A}\ ^2\Pi_u$ state of the CS_2^+ ion. The assignments for the PHOFEX spectrum were given in Figure 2 and Table 1. As indicated in Figure 2 and Table 1, the observed

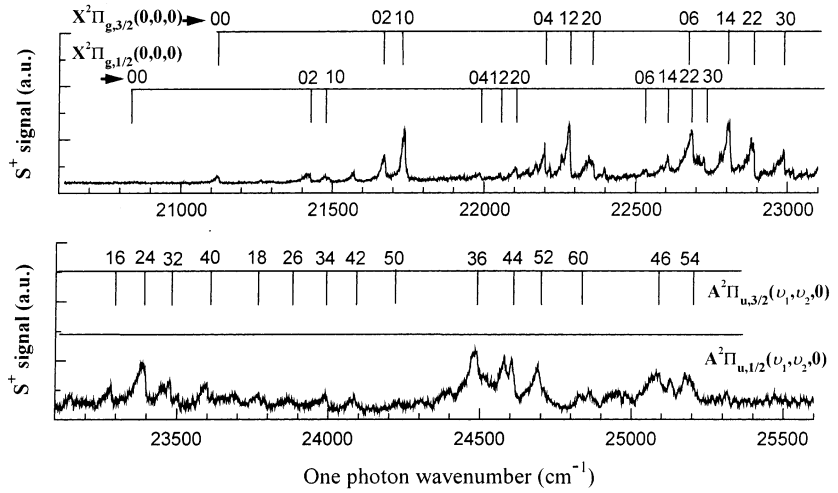

Figure 2. PHOFEX spectrum obtained by monitoring S^+ ions in the wavelength range of 385−485 nm. The spectrum was assigned to two series of $\tilde{A}\ ^2\Pi_{u,3/2}(\nu_1,\nu_2,0) \leftarrow \tilde{X}\ ^2\Pi_{g,3/2}(0,0,0)$ and $\tilde{A}\ ^2\Pi_{u,1/2}(\nu_1,\nu_2,0) \leftarrow \tilde{X}^2\Pi_{g,1/2}(0,0,0)$ vibronic transitions of the CS_2^+ ion, indicating that the S^+ ions were generated from the $\tilde{A}$-state-intermediated two-photon dissociation process of the CS_2^+ parent ions by the dissociation laser. The spectrum was not corrected for the laser energy.

TABLE 1: Wavenumbers and Vibrational Assignments for the $CS_2^+(\tilde{A}^2\Pi_u(\nu_1,\nu_2,0)) \leftarrow CS_2^+(\tilde{X}^2\Pi_g(0,0,0))$ Transitions

$\leftarrow \tilde{X}^2\Pi_{g,3/2}(0,0,0)$ $\tilde{A}^2\Pi_{u,3/2}(\nu_1,\nu_2,0)$	ν_{exp} (cm^{-1})	spacing (cm^{-1})	$\leftarrow \tilde{X}^2\Pi_{g,1/2}(0,0,0)$ $\tilde{A}^2\Pi_{u,1/2}(\nu_1,\nu_2,0)$	ν_{exp} (cm^{-1})	spacing (cm^{-1})
000	21121.9	0	000	20835.3	0
020	21671.4	549.5	020	21420.8	585.5
100	21736.8	614.9	100	21477.9	642.6
040	22199.8	1077.9	040	21984.8	1149.5
120	22280.3	1158.4	120	22054.0	1218.7
200	22348.7	1226.8	200	22106.1	1270.8
060	22684.2	1562.3	060	22535.7	1700.4
140	22806.2	1684.3	140	22606.7	1771.4
220	22879.2	1757.3	220	22684.2	1848.9
300	22987.2	1865.3	300	22724.1	1888.8
160	23283.9	2162.0			
240	23383.2	2261.3			
320	23475.6	2353.7			
400	23598.1	2476.2			
180	23767.1	2645.2			
260	23869.0	2747.1			
340	23990.8	2868.9			
420	24085.3	2963.4			
500	24234.1	3112.2			
360	24483.3	3361.4			
440	24603.4	3481.5			
520	24690.3	3568.4			
600	24865.9	3744.0			
460	25080.3	3958.4			
540	25190.9	4069.0			

resonance peaks in the spectrum correspond to transitions from the (0,0,0) vibrational levels[2,27] in the $\tilde{X}^2\Pi_{g,3/2}$ state to the $\nu = 0-7$ vibrational levels in the $\tilde{A}\ ^2\Pi_{u,3/2}$ state and to transitions from the (0,0,0) vibrational levels in the $\tilde{X}^2\Pi_{g,1/2}$ states to the $\nu = 0-3$ vibrational levels in the $\tilde{A}\ ^2\Pi_{u,1/2}$ states, where ν represents a group of vibrational levels coupled through Fermi resonance interaction and is defined as $\nu = \nu_1 + (\nu_2/2)$ (here, ν_1 and ν_2 denote vibrational quantum numbers for the ν_1 (symmetric stretch) and ν_2 (bend) modes, respectively). Interestingly, Figure 2 shows that the intensities of the transition progression of $\tilde{A}\ ^2\Pi_{u,1/2}(\nu_1,\nu_2,0) \leftarrow \tilde{X}\ ^2\Pi_{g,1/2}(0,0,0)$ is much weaker than that of $\tilde{A}\ ^2\Pi_{u,3/2}(\nu_1,\nu_2,0) \leftarrow \tilde{X}\ ^2\Pi_{g,3/2}(0,0,0)$. This can be explained, at least, by the strong population of $\tilde{X}^2\Pi_{g,3/2}(0,0,0)$ and the weak population of $\tilde{X}^2\Pi_{g,1/2}(0,0,0)$ with the [3+1] REMPI of the CS_2 at the ionization laser wavelength of $\lambda_1 = 483.2$ nm.[27]

(B) Adiabatic Appearance Potential of CS^+. Until now, several "indirect" methods were used to deduce the adiabatic appearance potential (AP) of the CS^+ ion. For example, CS^+ AP values of 16.16, 15.8, and 15.8 eV above the vibrationless ground state of CS_2 were given by electron impact ionization (from Momigny et al.[12]), energy transfer of the Ar^+ ion to CS_2 (from Shukla et al.[28]), and photoelectron−photoion coincidence (PEPICO) spectroscopy (from Aitchison and Eland[29]), respectively. In this work, it is shown that the yield of CS^+ ion obviously increases at a two-photon energy position of ~47 200 cm^{-1}, as shown in Figure 3. The population of $CS_2^+(\tilde{X}^2\Pi_{g,1/2}(0,0,0))$ is much less than that of $CS_2^+(\tilde{X}^2\Pi_{g,3/2}(0,0,0))$ in the [3+1] REMPI process[27] by ionization laser, and around the appearance position of the CS^+ ion there is a remarkable resonance band that was assigned to the one-photon transition of $\tilde{A}^2\Pi_{u,3/2}(4,0,0) \leftarrow \tilde{X}^2\Pi_{g,3/2}(0,0,0)$ (as

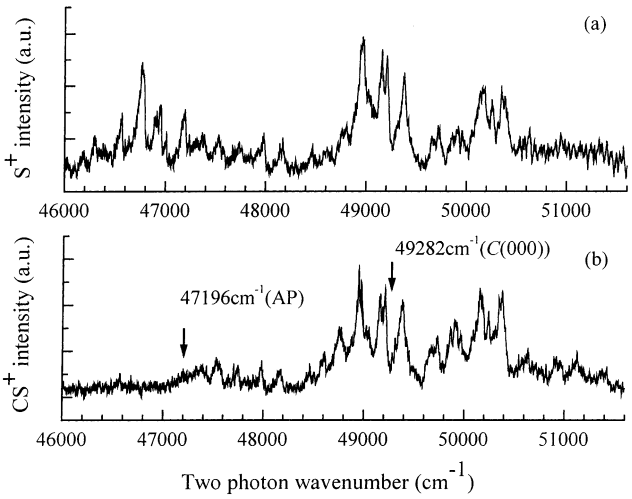

Figure 3. PHOFEX spectra obtained by monitoring (a) S^+ ions and (b) CS^+ ions in the range of 46000−51600 cm^{-1} (two-photon energy). The two arrows in panel b indicate the position of the appearance potential (AP) of the CS^+ ion (at 47 196 cm^{-1}) and that of the $\tilde{C}$(000) level of the CS_2^+ ion (at 49 282 cm^{-1}).

shown in Figure 2 and Table 1); therefore, it is reasonable to determine the AP value of the CS^+ ion as 47 196 ± 40 cm^{-1} above the $CS_2^+(\tilde{X}^2\Pi_{g,3/2}(0,0,0))$ level, as shown in Figure 3. Obviously, this method to excite the CS_2^+ parent ion directly can give a more precise and reliable value of CS^+ adiabatic appearance potential (that is, 5.852 ± 0.005 eV above the $CS_2^+(\tilde{X}^2\Pi_{g,3/2}(0,0,0))$ level, or 15.930 ± 0.005 eV above the $CS_2(\tilde{X}(000))$ level). Although the photodissociation laser has a spectral resolution of <0.1 cm^{-1}, we only give the values with a large uncertainty of ±40 cm^{-1}, because of the precision necessary to determine the appearance position of the CS^+ ion in the CS^+ PHOFEX spectrum.

Note that the CS^+ appearance potential of 47 196 cm^{-1} is lower than 49 282 cm^{-1}, which is the energy position of the $CS_2^+(\tilde{C}^2\Sigma_g^+(000))$ level,[21] as shown in Figure 3. This observation means that the appearance of the CS^+ ion does not need to proceed via the $CS_2^+(\tilde{C}^2\Sigma_g^+)$ level and follow coupling between the $\tilde{C}$ electronic state and the $^4\Sigma^-$ or/and $^2\Sigma^-$ repulsive state. The concerned dissociation mechanics to produce CS^+ below the $\tilde{C}$ electronic state of the CS_2^+ ion will be discussed in the following.

(C) [1+1] Photodissociation Mechanism. In Figure 3, the S^+ and CS^+ PHOFEX spectra obtained by monitoring the S^+ and CS^+ species simultaneously were given, versus the two-photon wavenumber. The CS^+ PHOFEX spectrum, in comparison to the S^+ PHOFEX spectrum, has a similar spectral structure, within the wavenumber range of 47 388−51 000 cm^{-1}, provided that the two-photon energy is larger than the AP value of the CS^+ ion.

Similar to our previous study for $CS_2^+ \rightarrow S^+ + CS$,[2] the proposed dynamics for the [1+1] photodissociation process of CS_2^+ to produce the CS^+ fragment ion can be described as follows. It is known that[12] the way to produce a CS^+ fragment ion from the CS_2^+ ion relies on the two-photon excitation to the two repulsive $^4\Sigma^-$ and $^2\Sigma^-$ states. Although the transition from the $\tilde{A}\ ^2\Pi_u$ state to the $^2\Sigma^-$ state is spin-allowed, the direct excitation from the $\tilde{A}\ ^2\Pi_u$ state to the $^4\Sigma^-$ state is spin-forbidden in the Hund's case (a) approximation, unless the $^4\Sigma^-$ state gains intensity via the spin−orbit interaction, which mixes the $^4\Sigma^-$ state and a spin-allowed electronic state. Balfour[13] and Maier and co-workers[21] have shown that the $\tilde{B}^2\Sigma_u^+(0,0,0)$ and $\tilde{C}^2\Sigma_g^+(0,0,0)$ levels are located at 35 460 cm^{-1} (4.40 eV) and 49 282 cm^{-1} (6.11 eV), respectively, above the $\tilde{X}^2\Pi_{g,3/2}(0,0,0)$ level of the CS_2^+ ion. However, in the energy range of the photodissociation laser (<6.11/2 eV), the two-photon excitation cannot energetically reach the $\tilde{C}^2\Sigma_g^+$ state[24] but can reach the energy region of high vibrational levels in the $\tilde{B}^2\Sigma_u^+$ state. In this energy region, the $^4\Sigma^-$ state may couple with the spin-allowed $\tilde{B}^2\Sigma_u^+$ state and, hence, gain some doublet character. Obviously, an electronic transition of the CS_2^+ ion from the $\tilde{A}\ ^2\Pi_u$ state to the linear excited state $\tilde{B}^2\Sigma_u^+$ is strongly forbidden in a one-photon excitation by the electric dipole selection rule. One plausible explanation is to consider the possibility of vibronic coupling. There are two possible ways for a forbidden electronic transition to gain intensity: by Herzberg−Teller intensity stealing, which would imply a breakdown of the Franck−Condon approximation, or by a breakdown of the Born−Oppenheimer approximation. The vibronic state can only mix with an allowed electronic state of the same symmetry, and the extent of the interaction is dependent on the separation of the two electronic states. For the $\tilde{B}^2\Sigma_u^+$ state, there are no possible electronic states to mix with, via vibronic interaction, whereas for the $\tilde{A}\ ^2\Pi_u$ state, there are the high vibrational levels of the $\tilde{X}^2\Pi_g$ state nearby to couple with.[12] Therefore, the intensity in this forbidden $\tilde{B}^2\Sigma_u^+ \leftarrow \tilde{A}^2\Pi_u$ transition comes from the vibronic coupling of $\tilde{A}^2\Pi_u$ and $(\tilde{X}\ ^2\Pi_g)^\dagger$, where the dagger symbol (†) represents high vibrational levels in the corresponding electronic states. Note that, in the first step of excitation of the CS_2^+ ion, it is not necessary to call for a complete relaxation to the $(\tilde{X}\ ^2\Pi_g)^\dagger$ state, followed by excitation to $\tilde{B}^2\Sigma_u^+$, because only the g → u → u sequence of the electronic inversion symmetries is needed to the transitions of $\tilde{X}^2\Pi_g \rightarrow \tilde{A}\ ^2\Pi_u \rightarrow \tilde{B}\ ^2\Sigma_u^+$. That is, the vibronic inversion symmetry that characterizes the $\tilde{A}\ ^2\Pi_u \rightarrow (\tilde{X}\ ^2\Pi_g)^\dagger$ coupling (u) will be conserved, regardless of the state they say the second step originates from. The final state must be vibronically g for the transition matrix element to be nonzero. This can only occur for a $\tilde{B}^2\Sigma_u^+$ final state if the overall transition from the original level in $\tilde{X}\ ^2\Pi_g$ is accompanied by an odd change in the bend or asymmetric stretch quantum number. According to the vibronic coupling theory[31] for a linear triatomic molecules of $D_{\infty h}$ symmetry, such as CS_2^+, with the ν_1 (Σ_g^+) symmetric stretching vibration, ν_2 (Π_u) bending vibration, and ν_3 (Σ_u^+) asymmetric stretching vibration, it could happen that one excites from the $\tilde{X}^2\Pi_g(0,0,0)$ level to the $\tilde{A}\ ^2\Pi_u(\nu_1,2m,2n)$ level and that this state couples resonantly with $(\tilde{X}\ ^2\Pi_g\ (\nu_1', 2m' + 1, 2n'))^\dagger$, where $m, n, m', n' = 0, 1, 2, ...$ These states both have u (most probably Π_u Renner) vibronic symmetry and can be simply regarded as a mixed state. Now, to excite to the $\tilde{B}^2\Sigma_u^+$ state, the only transitions allowed are those that terminate on an odd-numbered bending level (which could be viewed as vertical in a sense or an even change from the coupled $\tilde{X}^\dagger$ component and different by an odd number from $\tilde{A}$; however, this distinction is unnecessary and is, in effect, lost in the vibronic interaction). A similar logic applies to transitions and coupling facilitated by excitation in an asymmetric stretch; that is, the $\tilde{A}\ ^2\Pi_u(\nu_1,2m,2n)$ level couples resonantly with the $(\tilde{X}^2\Pi_g(\nu_1',2m',2n' + 1))^\dagger$, where $m, n, m', n' = 0, 1, 2, ...$ These states also both have u vibronic symmetry and can be simply regarded as a mixed state. Moreover, the coupling of the $\tilde{B}^2\Sigma_u^+$ state and the $^2\Sigma^-$ repulsive state, which lies a little higher than the $^4\Sigma^-$ repulsive state, in regard to energy, should also give its contribution to the CS^+ fragmentation process of the CS_2^+ ion in the shorter wavelength. In sum, the first excitation step in the [1+1] dissociation process to generate CS^+ fragments is the CS_2^+ $(\tilde{A}^2\Pi_u) \leftarrow CS_2^+(\tilde{X}^2\Pi_g)$ transition, followed by the $CS_2^+(\tilde{B}^2\Sigma_u^+) \leftarrow CS_2^+$ $(\tilde{A}^2\Pi_u)$ transition (which comes from the

vibronic coupling between CS_2^+ ($\tilde{A}^2\Pi_u$) and $CS_2^+(\tilde{X}^2\Pi_g)^\dagger$ by the $\nu_2(\Pi_u)$ bending vibration or the $\nu_3(\Sigma_u^+)$ stretching vibration); finally, CS_2^+ dissociates to $CS^+(X\,^2\Sigma) + S(^3P)$ via the coupling of $\tilde{B}\,^2\Sigma_u^+$ with the repulsive $^4\Sigma^-$ state or/and $^2\Sigma^-$ state. This dissociation process can be expressed as

$$CS_2^+(\tilde{X}^2\Pi_g) \xrightarrow{h\nu} CS_2^+(\tilde{A}^2\Pi_u) \quad (1)$$

$$CS_2^+(\tilde{A}^2\Pi_u) \xrightarrow{\text{vibronic interaction}} CS_2^+(\tilde{X}^2\Pi_g)^\dagger \quad (2)$$

$$CS_2^+(\tilde{X}^2\Pi_g)^\dagger \xrightarrow{h\nu} CS_2^+(\tilde{B}^2\Sigma_u^+) \quad (3)$$

$$CS_2^+(\tilde{B}^2\Sigma_u^+) \xleftarrow{\text{spin orbit}} CS_2^+(^4\Sigma^-) \quad (4)$$

$$CS_2^+(\tilde{B}^2\Sigma_u^+) \xleftarrow{\text{coupling}} CS_2^+(^2\Sigma^-) \quad (5)$$

$$CS_2^+(^4\Sigma^-, {}^2\Sigma^-) \rightarrow CS^+(X\,^2\Sigma) + S(^3P) \quad (6)$$

Note that the direct transitions to repulsive states, which have built-in stretch asymmetry, offer another way to excite from $\tilde{A}\,^2\Pi_u$ to an ungerade electronic configuration. This is implied in the coupling suggested between $\tilde{B}^2\Sigma_u^+$ and the repulsive $^2\Sigma^-$ and $^4\Sigma^-$ states. Although vibronic coupling at both the first- and second-photon levels seems very reasonable and would serve well to explain the postulated photophysics, we should not discount the possibility of electronic transitions that are fully allowed in case there is not a $^2\Sigma_g$ or $^2\Pi_g$ state in the region of the second-photon energy. Baltzer et al.[24] have shown that a weak satellite state (marked 1′ in Figure 5 of ref 24), apparently based on a $2\pi_u$ hole with another electron excited, is located at the blue side of the $\tilde{B}$ state and may overlap with the region above the Franck−Condon zone of the $\tilde{B}$ state. This satellite state is likely into the region of the CS^+ threshold and might easily be an allowed optical transition from the $\tilde{A}$ state itself. Thus, it is possible that this may be at least as likely a route to the products of CS^+ and S as the explanation proposed previously, which involves a dipole-forbidden absorption.

The branching ratio is an important parameter to study the photodissociation dynamics. By PEPICO measurement, a branching ratio of 55% ± 15% to CS^+/CS_2^+ and a S^+/CS^+ ratio of 57/43 were given in the dissociation of the CS_2^+ ion around the $\tilde{C}$ state by Brehm and co-workers[20] and Aitchson and Eland,[29] respectively. Figure 3 of ref 20 showed that, from ~15.8 eV, the CS^+ ions appear and the branching ratio increased to ~1 at 16.3 eV. Hwang et al.[23] measured the product branching ratio (CS^+/S^+) in the study of the predissociation of $CS_2^+(\tilde{C}\,^2\Sigma_g^+)$ and found that (i) the branching ratios of CS^+/S^+ are 0.79 ± 0.01 for the $\tilde{C}(000)$ level and 1.00−1.09 for other vibrationally excited levels of the $\tilde{C}$ state and (ii) the CS^+/S^+ value for bend vibration levels is slightly larger than that for the levels with a symmetry stretching vibration. In this report, the branching ratio of CS^+/S^+ was given in the range of 47 000−50 600 cm^{-1} (two-photon energy) and is shown in Figure 4. Although there seems a small plateau in the range of 47 500−48 200 cm^{-1}, where the branching ratio of CS^+/S^+ is ~33% totally, the branching ratio of CS^+/S^+ increases from 0 at 47 200 cm^{-1} to slightly larger than 1 at ~50 400 cm^{-1}. This result is not only similar in energy to that measured at the $\tilde{C}$ state by Hwang et al.,[23] but also is agreement with that given in the PEPICO experiment conducted by Aitchson and Eland.[29]

What is the relation between the dissociation to $CS^+ + S$ and the excitation of the $\tilde{C}$ state? In our case, a two-photon transition from $\tilde{X}$ to $\tilde{C}$ is impossible; because of the low intensity and the weak focusing of photodissociation laser, the [1+1] transition of $\tilde{C} \leftarrow \tilde{A} \leftarrow \tilde{X}$ is almost impossible, because one laser wavelength hardly satisfies the vibration transition between $\tilde{C} \leftarrow \tilde{A}$ and that between $\tilde{A} \leftarrow \tilde{X}$ simultaneously. Thus, the dissociation to $CS^+ + S$ seems to have a weak correlation to the $\tilde{C}$ state. That is, the dissociation to $CS^+ + S$ may be primarily dependent on both the Franck−Condon factor of $CS_2^+(\tilde{X}^2\Pi_g)^\dagger \xrightarrow{h\nu} CS_2^+(\tilde{B}^2\Sigma_u^+)$ transition and the overlap between the $\tilde{B}$ state and the repulsive $^4\Sigma^-$ state or/and $^2\Sigma^-$ state. Further detailed data on the electronic states of CS_2^+ is needed to explain that the dissociation probability to $CS^+ + S$ increases as the two-photon potential of the dissociation laser increases, as shown by the branching ratio of CS^+/S^+ in Figure 4.

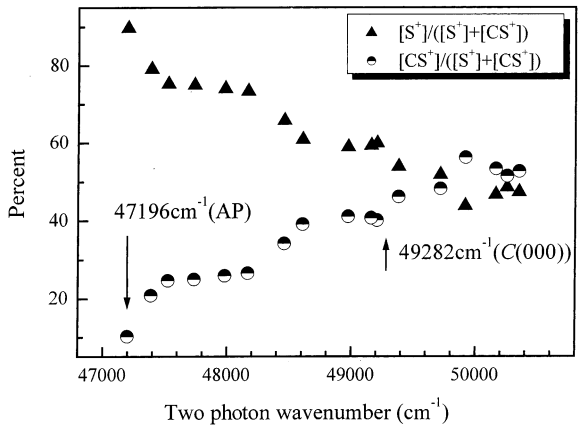

Figure 4. Percentage branching to each product ion in the range of 47 000−50 600 cm^{-1}. Two arrows indicate the position of the appearance potential (AP) of the CS^+ ion (at 47 196 cm^{-1}) and that of the $\tilde{C}(000)$ level of the CS_2^+ ion (at 49 282 cm^{-1}).

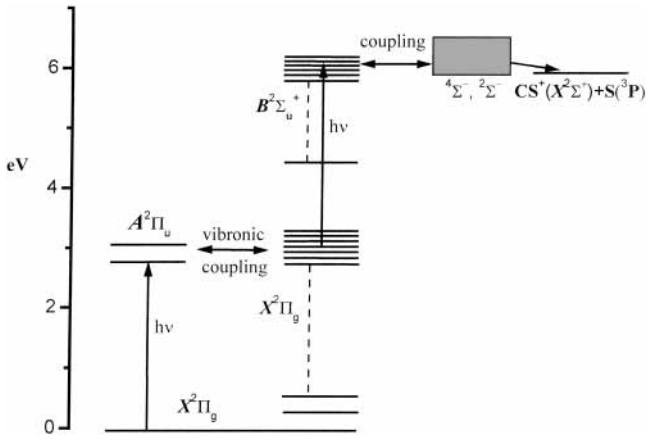

Figure 5. Schematic energy level diagram of the CS_2^+ ion, modified from refs 12, 13, and 21, with possible interactions among the electronic states, to illustrate the [1+1] excitation and dissociation process.

Figure 5 schematically shows the relevant potential levels of the CS_2^+ ion, modified from refs 12, 13, and 21, as well as the possible interactions among the electric states in the [1+1] excitation and dissociation processes.

Summary

The second dissociation channel ($CS_2^+ \rightarrow CS^+(X\,^2\Sigma) + S(^3P)$) of CS_2^+ molecular ions has been investigated by measuring the photofragment CS^+ excitation (PHOFEX) spectrum in the wavelength range of 385−435 nm. The adiabatic appearance potential of the CS^+ ion was determined to be 5.852 ± 0.005 eV above the $\tilde{X}\,^2\Pi_{g,3/2}(0,0,0)$ level of the CS_2^+ ion from the initial wavelength of 423.8 nm to produce the CS^+ ion. The

CS^+ PHOFEX spectrum, in a wavelength range less than the initial wavelength (423.8 nm) needed to produce the CS^+ ion, can be assigned essentially to the $CS_2^+(\tilde{A}\ ^2\Pi_u) \leftarrow CS_2^+(\tilde{X}^2\Pi_g)$ transition, similar to the S^+ PHOFEX spectrum.[2] The product branching ratios (CS^+/S^+), as measured from the PHOFEX spectra, increase from 0 to slightly larger than 1 in the range of 47 200−50 400 cm^{-1} (two-photon energy). The dissociation mechanism to obtain $CS^+ + S$ from CS_2^+ was discussed and was preliminarily attributed to (i) $CS_2^+(\tilde{X}^2\Pi_g) \rightarrow CS_2^+(\tilde{A}\ ^2\Pi_u)$ through one-photon excitation, (ii) $CS_2^+(\tilde{A}\ ^2\Pi_u) \rightarrow CS_2^+(\tilde{X}^\dagger)$ via an internal conversion process (because of the vibronic coupling between the $\tilde{A}$ state and the $\tilde{X}$ state, which enhances the efficiency of the second excitation step), (iii) $CS_2^+(\tilde{X}^\dagger) \rightarrow CS_2^+(\tilde{B}^2\Sigma_u^+)$ through the second photon excitation, and (iv) $CS_2^+(\tilde{B}^2\Sigma_u^+) \rightarrow CS^+(X\ ^2\Sigma) + S(^3P)$, because the energy curve crossing with the repulsive $^4\Sigma^-$ state and/or $^2\Sigma^-$ state correlated with the second dissociation limit.

Acknowledgment. Support from the National Natural Science Foundation of China (No. 20373067), and the National Key Basic Research Special Foundation (No. G1999075304) is gratefully acknowledged.

Note Added after ASAP Posting. This article was released ASAP on 2/3/2004. A data change was made in the caption of Figure 3. The correct version was posted on 2/6/2004.

References and Notes

(1) Hudson, R. D. *Rev. Geophys. Space Phys.* **1970**, *9*, 305.
(2) Zhang, L.; Chen, J.; Xu, H.; Dai, J.; Liu, S.; Ma, X. *J. Chem. Phys*. **2001**, *114*, 10768.
(3) Laird, R. K.; Barrow, R. F. *Proc. Phys. Soc., London, Sect. A* **1950**, *63*, 412.
(4) Callomon, J. H. *Proc. R. Soc. London, Ser. A* **1958**, *244*, 220.
(5) Leach, S. *J. Chim. Phys. Phys.−Chim. Biol*. **1964**, *61*, 1493; **1970**, *67*, 74.
(6) Eland, J. H. D.; Danby, C. J. *Int. J. Mass Spectrom. Ion Phys.* **1968**, *1*, 111.
(7) Brundle, C. R.; Turner, D. W. *Int. J. Mass Spectrom. Ion Phys*. **1969**, *2*, 195.
(8) Frost, D. C.; Lee, S. T.; McDowell, C. A. *J. Chem. Phys.* **1973**, *59*, 5484.
(9) Lee, L. C.; Judge, D. L.; Ogawa, M. *Can. J. Phys.* **1975**, *53*, 1861.
(10) Frey, R.; Gotchev, B.; Peatman, W. B.; Pollak, H.; Schlag, E. W. *Int. J. Mass Spectrom. Ion Phys*. **1978**, *26*, 137.
(11) Wang, L. S.; Reutt, J. E.; Lee, Y. T.; Shirley, D. A. *J. Electron Spectrosc. Relat. Phenom*. **1988**, *47*, 167.
(12) Momigny, J.; Mathieu, G.; Wankenne, H. *Chem. Phys. Lett*. **1973**, *21*, 606.
(13) Balfour, W. J. *Can. J. Phys.* **1976**, *54*, 1969.
(14) Ajello, J. M.; Srivastava, S. K. *J. Chem. Phys*. **1981**, *75*, 4454.
(15) Tokue, I.; Shimada, H.; Masuda, A.; Ito, Y. *J. Chem. Phys.* **1990**, *93*, 4812.
(16) Coxon, J. A.; Marcoux, P. J.; Setser, D. W. *Chem. Phys.* **1976**, *17*, 403.
(17) Yencha, A. J.; Wu, K. T. *Chem. Phys*. **1980**, *49*, 127.
(18) Tsuji, M.; Mizukami, K.; Sekiya, H.; Obase, H.; Shimada, S.; Nishimura, Y. *Chem. Phys. Lett*. **1984**, *107*, 389.
(19) Endoh, M.; Tsuji, M.; Nishimura, Y. *Chem. Phys. Lett*. **1984**, *109*, 35.
(20) Brehm, B.; Eland, J. H. D.; Frey, R.; Kustler, A. *Int. J. Mass Spectrom. Ion Phys*. **1973**, *12*, 213.
(21) Danis, P. O.; Wyttenbach, T.; Maier, J. P. *J. Chem. Phys*. **1988**, *88*, 3451.
(22) Evard, D. D.; Wyttenbach, T.; Maier, J. P. *J. Phys. Chem*. **1989**, *93*, 3522.
(23) Hwang, W. G.; Kim, H. L.; Kim, M. S. *J. Chem. Phys*. **2000**, *113*, 4153.
(24) Baltzer, P.; Wannberg, B.; Lundqvist, M.; Karlsson, L.; Holland, D. M. P.; MacDonald, M. A.; Hayes, M. A.; Tomasello, P.; von Niessen, W. *Chem. Phys*. **1996**, *202*, 185.
(25) Baker, J.; Konstantaki, M.; Couris, S. *J. Chem. Phys*. **1995**, *103*, 2436.
(26) Huang, J. C.; Cheung, Y. S.; Evans, M.; Liao, C. X.; Ng, C. Y.; Hsu, C. W.; Heimann, P.; Lefebvre-Brion, H.; Cossart-Magos, C. *J. Chem. Phys*. **1997**, *106*, 864.
(27) Morgan, R. A.; Baldwin, M. A.; Orr-Ewing, A. J.; Ashfold, M. N. R.; Buma, W. J.; Milan, J. B.; de Lange, C. A. *J. Chem. Phys*. **1996**, *104*, 6117.
(28) Shukla, A. K.; Tosh, R. E.; Chen, Y. B.; Futrell, J. H. *Int. J. Mass Spectrom. Ion Process.* **1995**, *146*, 323.
(29) Aitchison, D.; Eland, J. H. D. *Chem. Phys*. **2001**, *263*, 449.
(30) Liu, J.; Hochlaf, M.; Ng, C. Y. *J. Chem. Phys*. **2003**, *118*, 4487.
(31) McHale, J. L. *Molecular Spectroscopy*; Pearson Education North Asia Limited and Science Press: 2002; p 341.